Study on Sliding Friction Characteristics of Magnetorheological Elastomer - Copper Pair Affected by Magnetic-Controlled Surface Roughness and Elastic Modulus

Rui Li
Chongqing University of Posts and Telecommunications
Di Wang
Chongqing University of Posts and Telecommunications
Xinyan Li
Chongqing University of Posts and Telecommunications
Ping-an Yang (yangpa@cqupt.edu.cn)
Chongqing University of Posts and Telecommunications https://orcid.org/0000-0002-8072-8506
Haibo Ruan
Chongqing University of Posts and Telecommunications
Mengjie Shou
Chongqing University of Posts and Telecommunications

Original Article

Keywords: Magnetorheological elastomers (MREs), Magnetic field, Surface roughness, Elastic modulus, Sliding friction

Posted Date: January 15th, 2021

DOI: https://doi.org/10.21203/rs.3.rs-146108/v1

Version of Record: A version of this preprint was published at Smart Materials and Structures on November 22nd, 2021. See the published version at https://doi.org/10.1088/1361-665X/ac3c05.

Title page

Study on sliding friction characteristics of magnetorheological elastomer - copper pair affected by magnetic-controlled surface roughness and elastic modulus

Rui Li, born in 1975, is currently a PhD candidate at *Chongqing University, China*. His current position is a professor in *Chongqing University of Posts and Telecommunications*. His main research interests include intelligent detection technology, friction control and intelligent mechanical structure system.
Tel: +86-135-94078659; E-mail: lirui_cqu@163.com

Di Wang, born in 1996, is currently a master candidate at *School of Automation, Chongqing University of Posts and Telecommunications, China*.
E-mail: 812996901@qq.com

Xinyan Li, born in 1995, is currently a master candidate at *School of Automation, Chongqing University of Posts and Telecommunications, China.*
E-mail: 459148593@qq.com

Ping-an Yang, born in 1989, is currently a PhD candidate at *Chongqing University, China*. His current position is a lecturer in *Chongqing University of Posts and Telecommunications*. His main research interests include intelligent biomimetic composite materials, flexible sensor, electromagnetic shielding material and structural design.
Tel: +86-151-23254645; E-mail: yangpa@cqupt.edu.cn

Haibo Ruan, born in 1984, is currently a PhD candidate at *Chongqing University, China*. His research interests include construction of flexible nanowire composite transparent electrode and its performance enhancement.
Tel: +86-136-47619849; E-mail: rhbcqu@aliyun.com

Mengjie Shou, born in 1993, is currently a PhD candidate at *Chongqing University, China*. His main research interests include intelligent detection technology, friction control and intelligent mechanical structure system.
E-mail: shoumj@cqupt.edu.cn

Corresponding author：Ping-an Yang　E-mail：yangpa@cqupt.edu.cn

ORIGINAL ARTICLE

Study on sliding friction characteristics of magnetorheological elastomer - copper pair affected by magnetic-controlled surface roughness and elastic modulus

Rui Li[1]• Di Wang[1]• Xinyan Li[1]• Ping-an Yang[1]• Haibo Ruan[2]• Mengjie Shou[1]

Received June xx, 201x; revised February xx, 201x; accepted March xx, 201x

Abstract: To optimize the online friction coefficient adjustment, it is necessary to study the parameter change features of the magneto-sensitive polymer and its influence on the friction characteristics under magnetic field. A series of isotropic magnetorheological elastomers (MREs) with different initial surface roughness were prepared, and a sliding friction platform with MRE - copper block pair was built to carry out magnetic-controlled friction characteristic experiment. Results show that the sliding friction coefficient of MRE decreases with the increase of the magnetic field, but the degree of reduction is quite different under different initial surface roughness and elastic modulus. When the initial surface roughness of MRE is between 0.5 - 2.5 μm and the ferromagnetic particles volume fraction is between 10% - 15%, its magnetic-controlled friction coefficient has the largest reduced value of 22.75%. Moreover, features of elastic modulus and surface topography under magnetic field were tested and analyzed. By combining with the single peak contact model and the friction binomial law, the relationship between the surface roughness and elastic modulus of MREs and the sliding friction force is deduced, and it is proved that the friction coefficient is affected by the coupling effect of surface roughness and elastic modulus. The magnetic-controlled elastic modulus is the key factor, which determines the overall downward trend of the friction coefficient of MREs. Magnetic-controlled surface roughness also plays an important role in the adjustable range of friction coefficient, and reducing the initial surface roughness can increase the magnetic-controlled friction coefficient adjustable range.

Keywords: Magnetorheological elastomers (MREs) • Magnetic field • Surface roughness • Elastic modulus • Sliding friction

1 Introduction

Exploring how to control friction and reduce wear has important engineering significance and value [1-3]. With the rapid development of intelligent mechanical equipment and robot, the demand for regulation and utilization of friction has changed from simply increasing or reducing friction to online reversible intelligent regulation. The traditional friction control methods (mechanical regulation, adding lubricant, surface texturing) cannot enough to meet this requirement [4-7], and this has stimulated the development of technology for changing the surface friction characteristics of devices by external excitations, which mainly includes electric fields [8, 9], magnetic fields [10] and temperature fields [11]. In those methods, electric field control requires a high voltage, with the safety risk, and temperature control needs a relatively long response time. Relatively speaking, the magnetic field control method takes into account both safety and rapid response [12], and it is one of the most promising regulation methods for controllable friction engineering applications.

The magnetorheological elastomer (MRE) is a new type of smart material prepared by dispersed micron-sized ferromagnetic particles into a polymer matrix [13]. Under the action of magnetic field, dynamic mechanical properties of MREs can produce reversible changes within milliseconds, and have been widely used in various types of adjustable vibration isolation systems [14-16]. Recently, scholars [17-20] have begun to study the friction

✉ Ping-an Yang
yangpa@cqupt.edu.cn
Haibo Ruan
rhbcqu@aliyun.com
[1] School of Automation, Chongqing University of Posts and Telecommunications, Chongqing 400065, China
[2] Chongqing Key Laboratory of Materials Surface & Interface Science, Chongqing University of Arts and Sciences, Chongqing 402160, China

characteristics of MREs, and found that the friction coefficient and wear resistance of MREs will be changed by an applied magnetic field. As a friction-controllable material, MREs can be applied to the key parts of mechanical structures, such as brake pads, conveyor belts, robot palms and rubber gaskets [21-23]. In order to achieve precise control, the sliding friction characteristics of MRE materials and their components in engineering applications, it is necessary to fully understand which factors will affect their friction characteristics after the applied magnetic field. Lee et al. [17] designed and built a sliding friction experimental platform to measure the friction characteristics of MREs in the presence or absence of magnetic field. The results show that when there is a suitable magnetic field, the friction coefficient of MREs is reduced by about 0.1, and the variation range is about 40%. Further, Lian et al. [18] tested the elastic modulus and friction of MREs prepared from different matrix materials. The experimental results show that by using the magnetic field, the four kinds of MREs have different elastic modulus, which leads to changes in friction properties. It can be inferred that the change of the elastic modulus to magnetic field may be an important reason for the magnetic-controlled friction. On this basis, our research group [19, 20] derived that there maybe some trend between the friction coefficient of the isotropic MREs and the elastic modulus by combining the elastic contact theory. Meanwhile, our research group [24] found that the surface morphology of the MREs also changed with the magnetic field, and the surface roughness can affect the friction characteristics. In addition to the mechanical properties of the contact surface, the topographical features of the surface and modulus are also important factors affecting the friction characteristics [25]. However, surface roughness and elastic modulus may not affect friction coefficient alone, and there may be some coupling relationship between the two factors, they are all worth to research and explore. Most of the existing researches have not involved and systematically studied the coupling change of the surface roughness and elastic modulus of MRE under the effect of magnetic field, and it is unclear how the surface roughness and elastic modulus coupled affect the friction properties of MREs. Therefore, it is necessary to deeply explore the influence of surface roughness and elastic modulus on the sliding friction characteristics of MRE under magnetic field.

In this study, a series of isotropic MRE samples with different initial surface roughness was prepared, and a sliding friction experimental platform was further built. Then, friction force measurement experiments were performed in the presence or absence of a magnetic field, and the optimal proportions of the MRE with different initial surface roughness were explored, and laid the foundation for revealing the mechanism. Moreover, a variety of characterization were performed on the material, and the experimental results that the coupling effects of two important factors namely elastic modulus and surface topography are theoretically analyzed from the macroscopic experimental. Finally, through the application of elastic mechanic equation and tribological equation, one magnetic-controlled sliding friction mechanism of the MREs was revealed, which will help to achieve precisely controllable sliding friction.

2 Experiment

2.1 Fabrication of MRE samples with different roughness

The initial surface topography of the MREs has a decisive influence on the magnetic field-controlled surface roughness, and even a completely opposite change [20]. Therefore, in the preparation process, isotropic MRE samples with different surface topography and different particle volume ratios were prepared by special treatment of the mold.

2.1.1 Raw materials

The raw materials used in this experiment mainly include the polymer matrix and the filler. The polymer matrix is polydimethylsiloxane (PDMS; Sylgard 184, Dow Corning, USA), which consists of part A and part B, with a mass ratio of 10:1. The filler is carbonyl iron powder (Beijing Xing Rong Yuan Technology Co., Ltd, China) whose diameter is about 3-5 μm and shape is spherical. In addition, the diluting agent used was two-methyl silicone oil with 50 cp (Dow Corning, USA).

2.1.2 Preparation of samples

During the preparation of isotropic MRE samples, the materials were weighed according to the ratios of the components as shown in Table 1. First, two-methyl silicone oil and the weighed component A of the PDMS are mixed and stirred to reduce the viscosity, and the ferromagnetic particles and the rubber matrix are sufficiently mixed. Then, the weighed CIPs are poured into the as-prepared mixture, and the ferromagnetic particles and the mixture are sufficiently mixed to uniformly disperse. After that, the component B of PDMS has been further added, and thoroughly stirred. Hereafter the mixture is ultrasonically to promote the bubble inside the mixture to float, and placed in a vacuum drying oven which the vacuum was 101 Pa to guarantee the bubbles were completely removed. In order to make the isotropic MREs have different initial surface topography, the 360 mesh and 12000 mesh sandpapers were

selected respectively, and the sandpaper is cut into a rectangle of 60 mm × 60 mm size, which is consistent with the internal dimensions of the mold, and the cut sandpaper is adhered to the bottom of the model through the adhesive. For the isotropic MREs, the mixture after removing the bubbles was directly poured into a mold, sealed and placed in a vacuum drying oven at 80 □ until solidification molding, and the specific operation flow is shown in Figure 1. It can be seen from the schematic diagram of the material preparation process that the isotropic MREs will form a certain initial surface topography after demolding.

Table 1 Composition of the isotropic MRE samples

Samples	Sandpapers	Sample number	CIPs (Vol %)	Part A of PDMS (g)	Part B of PDMS (g)	CIPs (g)
Samples with smooth initial surface (S-MRE)	12000 mesh	1	5%	40	4	15.149
		2	10%	40	4	31.981
		3	15%	40	4	50.794
		4	20%	40	4	71.958
Samples with rough initial surface (R-MRE)	360 mesh	5	5%	40	4	15.149
		6	10%	40	4	31.981
		7	15%	40	4	50.794
		8	20%	40	4	71.958

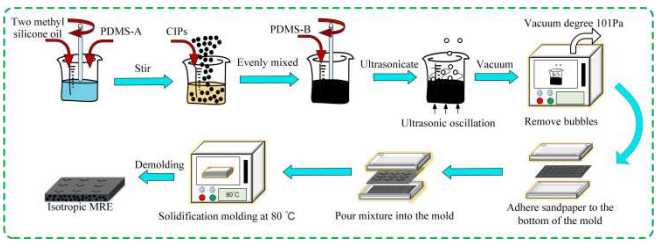

Figure 1 The preparation process of isotropic MRE samples with different roughness

2.2 Characterizations

According to the above preparation process, the isotropic MRE samples with different initial roughness were prepared, and two MRE samples 2 and 6 with the particle volume ratio of 10% were selected. Because when the volume fraction of ferromagnetic particles is 10%, the roughness of MRE changes more obviously [19]. An atomic force microscopy (AFM) image was taken with an NT-MDT NTEGRA Prima series atomic force microscope (Precision: Resolution can reach 1-3 μm; scanning range up to 200 μm × 200 μm) to characterize the microscopic surface morphology of MRE samples with different roughness. In short, first put the sample fixed on the iron sheet into the center of the magnetic sample table, so that it can attract the iron sheet and the sample. Then adjust the position of the optical microscope lens and adjust the four-quadrant detector. Finally, after initialling the scan parameters, scan the image and observe the microstructure.

A stylus contact measurement method was used to characterize the presence or absence of the one-dimensional contour of samples under a magnetic field. A surface roughness tester (TR210, Chongqing Libo Instrument Co., Ltd., China) with an accuracy of up to 0.001 was used for measurement. The rocker behind the fixed gantry was shaken to ensure that the probe of the surface roughness meter came into contact with the surface of the MRE sample, and the surface roughness meter can begin measuring.

A microcomputer-controlled electromechanical universal testing machine (TSE-104B, Shenzhen Wance Testing Machine Co., Ltd., China) was applied to characterize the elastic modulus of the two MRE samples 2 and 6. In short, a sample was placed in the middle of the electromagnet base, which was pressed with the machine's compression fixture and the machine's program was set up. In the case of different currents, the MRE sample was covered under different magnetic fields, and the compressive force data and the deformation degree at one time were measured with 2 min of reciprocating compression. Young's modulus was calculated by taking the average of the effective values obtained through multiple tests.

2.3 Experimental setup

2.3.1 Construction of the sliding friction test platform

A sliding friction experiment platform based on the friction pair of copper blocks was designed and built. The experimental platform is mainly composed of stepping motor, linear guide, tensile pressure sensor, pressure variable device, magnetic field applying device and a base. The principle and physical diagram of the experimental platform are shown in Figure 2. The surface friction force of the MREs is mainly tested by the planar constant force method. During the experiment, different positive pressures are provided by placing different numbers of copper blocks in the pressure variable device, and the stepping motor in the horizontal direction is driven to move at a uniform speed, so that the non-magnetic copper friction pair performs sliding friction on the MRE surface. The dimension of the friction force is output by the pulled pressure sensor. By placing a permanent magnet in the magnetic box and adjusting the magnetic field through the lifting device, the value of the friction force under different magnetic field can be measured. According to the experimental requirements, the sliding friction characteristics of MRE samples with different roughness before and after the application of a magnetic field were tested. In order to ensure the accuracy of the test results, each experiment test is repeated five times, and the average values are taken as the experimental result.

2.3.2 Friction force test method

The test procedure was designed as follows: First, after the top surfaces of MREs were wiped with alcohol to remove impurities (e.g., dirt and debris), the test sample was fixed on the top of the magnet box, thereby driving the horizontal motor to move the pressure variable device to the right. The entire process is a uniform rectilinear motion. Second, contact force data for the whole process were acquired by using the sensor and recorded with data acquisition software. Finally, loading was stopped when driving for 180 s and ended the test.

In the test, the force when the top surface of the test sample hindered the pressure variable device was regarded as the friction force of the MRE. Before the experiment, the permanent magnet was placed on the lifting device in the magnet box to explore the influence of different magnetic field strength on the sliding friction characteristics. The test was performed at a fixed pushing speed of 0.2 mm/s, different positive pressures (0.95 N, 1.92 N, 2.89 N, 3.86 N, 4.81 N) and different magnetic field intensities (0, 250 mT) and samples (Table 1). Each experiment was performed five times under the same condition, and the mean value was denoted as the final value. Figure 3 shows the raw data for the pushing time and friction force curve of sample 7.

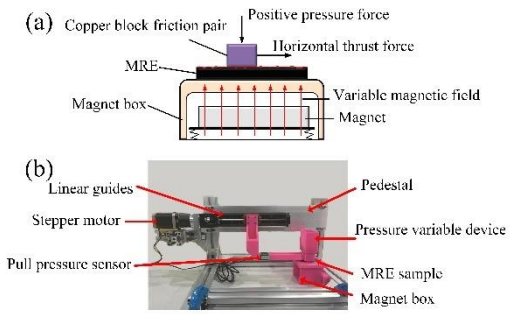

Figure 2 Measurement principle of MRE sliding friction characteristics and physical diagram of platform: (a) Schematic diagram of sliding friction test; (b) MRE sliding friction test platform

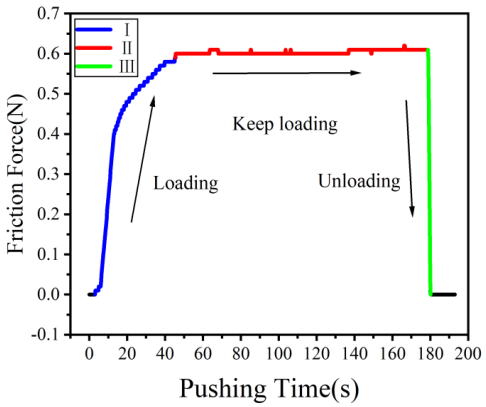

Figure 3 Pushing time and friction force curve of sample 7 when the positive pressure is 0.95 N: (□) Loading period; (□) Keep loading period; (□)Unloading period

3 Results and discussion

3.1 MRE sliding friction characteristics test results

Using the above-mentioned friction test platform, the prepared MRE samples were measured for surface friction force in positive pressures of 0.95 N, 1.92 N, 2.89 N, 3.86 N, 4.81 N and magnetic fields of 0 mT and 250 mT, respectively. The experimental results show that under different positive pressure conditions, the sliding friction characteristics of MREs under the applied magnetic field are consistent, as shown in Figure 4(a) - (d). In order to show more clearly, the experimental data in which the positive pressure is 2.89 N is analyzed and processed, and the specific change of the MRE friction coefficient under the action of the magnetic field is obtained, as shown in Figure 4(e) and 4(f).

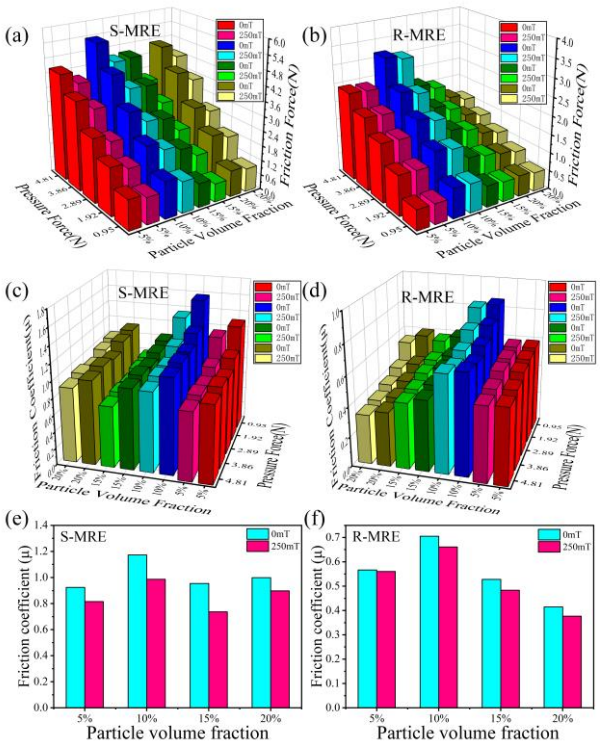

Figure 4 Results of MRE friction experiments with different roughness: (a) Friction force of S-MRE samples; (b) Friction force of R-MRE samples; (c) Friction coefficient of S-MRE samples; (d) Friction coefficient of R-MRE samples; (e) Friction coefficient of S-MRE samples when the positive pressure is 2.89 N; (f) Friction coefficient of R-MRE samples when the positive pressure is 2.89 N

The friction coefficient of MREs before and after application of magnetic field is obtained by Coulomb's law $\mu = f/P$, f is friction force and P is positive pressure

force. It can be found that in the absence of magnetic field, the MREs with different initial morphologies exhibit different friction coefficients, and the friction coefficient of the S-MRE samples is larger than that of the R-MRE samples. This result shows that the surface roughness and friction force of MREs are correlated, and there has a certain suitable initial surface roughness that can help to reduce the friction coefficient. Under a magnetic field of 250 mT, the friction coefficient of each MRE sample has changed to different extent. In general, the magnetic field can control the reduction of the friction coefficient of the MREs. Further, the change degree of the friction coefficient under and without the magnetic field was compared and analyzed, and the results are shown in Table 2.

Table 2 Comparison of MRE friction coefficient before and after applying magnetic field with a positive pressure of 2.89N

Samples	Sample number	CIPs (Vol %)	μ under magnetic field of 0 mT	μ under magnetic field of 250 mT	Rate of change (%)
Samples with smooth initial surface	1	5%	0.9241	0.8154	11.76
	2	10%	1.1729	0.9860	15.90
	3	15%	0.9539	0.7369	22.75
	4	20%	0.9984	0.8976	10.10
Samples with rough initial surface	5	5%	0.5668	0.5604	1.12
	6	10%	0.7053	0.6610	6.25
	7	15%	0.5281	0.4833	8.48
	8	20%	0.4144	0.3770	9.04

It can be seen from Table 2 that the MRE samples with different initial roughness have a significant difference in change rate of the friction coefficient under magnetic field. Under the same other conditions, the decreasing trend of μ of S-MRE is as the volume ratio first increases and then decreases, and the decreasing trend of μ of R-MRE is increasing as the volume ratio increases. A possible reason is that with the increase of ferromagnetic particles, the change of the elastic modulus under the magnetic field gradually increases, and the rate of change may decrease after a certain volume fraction [26]. The changing trend of the elastic modulus and that of the friction coefficient are almost in an inverse relationship, so whether there is a certain connection and influence between the two parameters. Under the magnetic field, the change of friction coefficient of the S-MRE samples observably more than the R-MRE samples, which may be caused by the different changes in the surface morphology of the two types samples with the magnetic field. Different surface roughness shows different friction coefficient change trend, which indicated that surface roughness can have some influence on the change of friction coefficient. When the volume fraction of S-MRE is 20%, the downward trend of friction coefficient slows down, but that of R-MRE still increases. It may be because the overall viscosity and other mechanical properties of MRE will increase when the volume fraction is 20%. When the surface is smooth, the influence of mechanical properties on the elastic modulus can be observed, and the upward trend of it decreases accordingly; when the surface is rough, the influence of mechanical properties on it is small due to the more convex surface, and the upward trend of it is still increasing. This also shows that elastic modulus and surface roughness are not a single effect on the friction coefficient, but a coupled influence on it. Therefore, choosing S-MRE with ferromagnetic particles volume of 10% - 15% can more stably obtain an excellent friction coefficient variation range, which can reach about 23%. For instance, under a magnetic field of 250 mT, the μ change rate of sample 3 which with a initial smooth surface can be up to 22.75%. While, under the same magnetic field, for R-MRE samples, the largest friction coefficient change rate is only 9.04%.

Since surface roughness is a very important factor of MRE magnetic-controlled friction parameters, so a series of surface topography tests and analyses were carried out. The AFM images of the two MRE samples 2 and 6 were taken in order to visually see the comparison of different initial surfaces. From the Figure 5(a) and 5(b), it can be seen that, the sandpaper of 12000 mesh was placed at the bottom of the mold, the surface of the prepared MREs is relatively smooth. While, after the sandpaper of 360 mesh was placed at the bottom of the mold, the surface of the prepared MREs is undulating and rough. It is indicated that the MRE samples with different initial morphology can be effectively prepared by treating the bottom of the mold with different meshes of sandpaper. In addition, the surface roughness tester was used to test the one-dimensional contour of samples under a magnetic field. It can be seen from Figure 5(d) and 5(e) that, when there is no magnetic field, the surface of S-MRE sample 2 is relatively flat, and the surface of R-MRE sample 6 has large undulations, and there are a large number of convex peaks. Under a magnetic field of 250 mT, the surface morphology and contours of the two samples changed greatly. The surface of S-MRE sample 2 produced a large number of convex peaks, and the surface unevenness increased compared to without magnetic field. On the contrary, the peak value of the surface convex peak of R-MRE sample 6 was weakened, compared without magnetic field, which the surface roughness is lower.

According to the statistical results shown in Figure 5(c), the surface roughness of the MRE sample with a relatively smooth initial surface will increase with the increase of the magnetic field. For example, the maximum surface roughness change rate of S-MRE samples increased up to

84.35% under a magnetic field of 250 mT. However, when the initial surface is rough, the surface roughness of MRE will decrease with the magnetic field. For instance, maximum drop rate of R-MRE samples can reach 27.61%. By comparing and analyzing the samples with different initial surface roughness, the experimental results show that the initial roughness of MRE samples with different particle volume fractions are different, and the changing trend of magnetic-controlled surface roughness is also different. This means that the initial surface roughness may be an important factor affecting of the magnetic-controlled sliding friction characteristics. Furthermore, it is worth mentioning that, no matter how large the initial roughness is, after applying the magnetic field, the roughness is close to the critical value of about 3 μm. The surface roughness of S-MRE which has a better friction coefficient is between 0.5 - 2.5 μm.

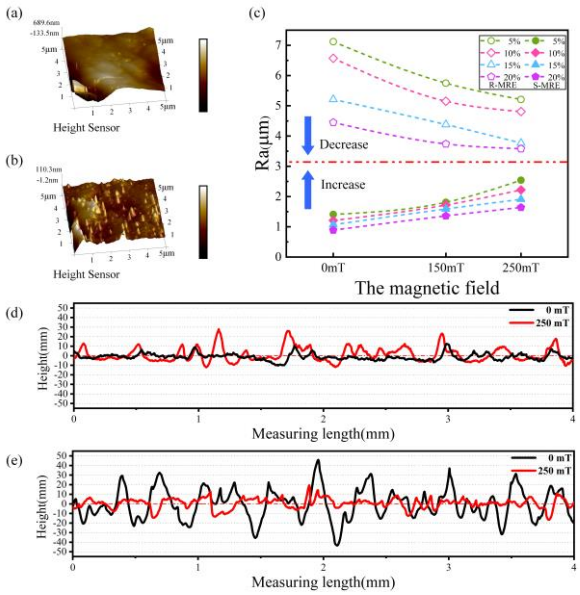

Figure 5 Surface profile comparison of MREs with different surface roughness: (a) AFM of S-MRE sample 2; (b) AFM of R-MRE sample 6; (c) Comparison of surface roughness changes of MRE samples 1-8 under magnetic field; (d) One-dimensional contour change of S-MRE sample 2 under magnetic field; (e) One-dimensional contour change of R-MRE Sample 6 under magnetic field

The elastic modulus is also an important factor affecting the magnetic-controlled sliding friction characteristics of MRE. For this reason, the elastic modulus of two MRE samples 2 and 6 were characterized by the instrument. The test generates different magnetic field strength by applying different drive currents in the coil, and the elastic modulus is the ratio of positive pressure to the deformation degree. It can be seen from Figure 6 that the different initial surface morphology of the MREs have little effect on the change of magneto-elastic modulus, and the elastic modulus of the samples all increase with the increase of the magnetic field. It shows that the elastic modulus of MRE has the characteristics of adjustable and controllable under the magnetic field. It will increase with the increase of the magnetic field and the material will become hardness. Varieties in mechanical contact characteristics affect its sliding friction characteristics. Under the same test conditions (force, displacement, magnetic field, and volume ratio), the elastic modulus of S-MRE and that of R-MRE showed slightly different values.

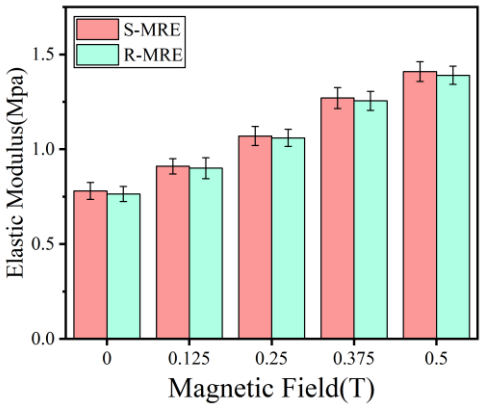

Figure 6 Elastic modulus of MRE samples 2 and 6 with different surface roughness

Generally, under the magnetic field, the elastic modulus of MRE sample has a high rate of change, which can increase 123% with the 20% particles volume fraction [26]. Meanwhile, when the initial surface of MRE is different, the surface roughness will increase or decrease with the increase of magnetic field. However, the friction coefficient of all MREs decreases as the magnetic field increases. Therefore, the main factor affecting the magnetic-controlled sliding friction characteristics of MRE may be that the modulus increases with the increase of magnetic field. The difference in magnetic-controlled surface roughness caused by different initial surface roughness may only change the degree of friction coefficient reduction. S-MRE samples increase the surface roughness under the magnetic field and enhance the reduction of friction coefficient. However, under the magnetic field, the surface roughness of R-MRE samples is reduced, which reduces the tendency of the friction coefficient to decrease. It can be assumed and inferred that there is a coupling relationship between the elastic modulus and roughness.

3.2 Theoretical analysis

Based on previous experimental research on friction

coefficient, surface roughness and elastic modulus, some inferences and results have been obtained which can be referenced. It is found that the magnetic-controlled friction mechanism of MRE is related to the two factors, and there may be a coupling relationship between the two factors to affect the friction coefficient together. Meanwhile, it is known that the surface morphology and mechanical properties of the object are important factors determining the friction characteristics [27]. In order to analyze the magnetic-controlled friction mechanism of MRE in principle, it is necessary to study the role and correlation between the surface topography and the elastic modulus from a theoretical analysis. The microstructure of the MRE was observed by a white light interferometer in the early stage. The results are shown in Figure 7.

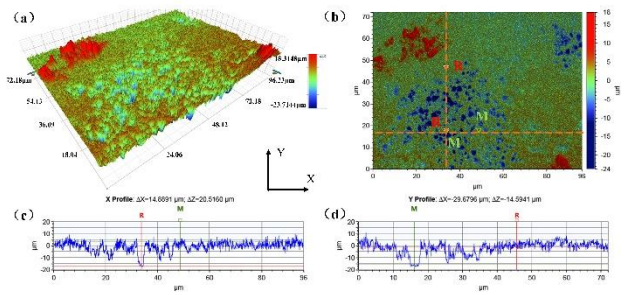

Figure 7 Observation results of surface morphology of MRE: (a) three-dimensional surface topography of MRE; (b) two-dimensional surface topography of MRE; (c) contour curve of MRE along the x-direction; d) contour curve of MRE along the y-direction

The results of white light interferometer test show that there are actually many microscopic peaks and valleys on the surface of the MRE sample which seemingly smooth. In the process of making contact with the friction pair, microscopically, the mutual contact of the two surfaces is actually the contact between the surface micro bulge.

It is assumed that the ideal initial surface topography of the MRE is composed of a number of rough peaks with neat rows, different height and the same radius. Under uniform stress, the rough peaks do not affect each other, and there is a critical point of initial surface roughness Ra_0.When the roughness is Ra_0, the number of peaks actually contacted is n_0. Introducing relative roughness k_0:

$$k_0 = \frac{Ra}{Ra_0} \tag{1}$$

Where Ra represents the surface roughness of the MRE. When $k_0 > 1$, it represents that the initial surface of the MRE is relatively rough. When $0 < k_0 < 1$, it represents that the initial surface of the MRE is relatively smooth. The actual contact position between the copper block and the MRE with different surface roughness under ideal conditions is shown in Figure 8.

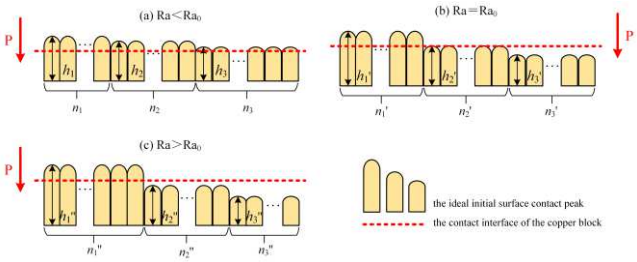

Figure 8 The different contact diagram of the ideal initial surface morphology of MRE and the surface of the copper block when pressed

The surface roughness Ra of the MRE mainly depends on the flatness of the surface topography. Small initial surface roughness indicates that the peak height of the surface of the MRE is small, and the height difference between the peaks is not obvious, as shown in Figure 8(a). On the contrary, large initial surface roughness indicates that the peak height of the surface of the MRE is large, and the height difference between the peaks is large, as shown in Figure 8(c). Since the peak height of the MRE is on the order of micrometers, which is much smaller than the overall thickness of the material, it is reasonable to assume that the elastic modulus of each contact peak is the same as the elastic modulus of the entire material. The actual contact area of the friction pair can be analyzed as follows, when the initial surface roughness is less than the critical value of Ra_0, all the rough peaks with heights h_1, h_2, and h_3 are in contact with the friction pair under the action of pressure, and the number of contacts is $n = n_1 + n_2 + n_3$. When the initial surface roughness is equal to the critical value of Ra_0, the number of rough peaks in contact is $n = n_0 = n_1' + n_2'$. However, when the initial surface roughness is greater than the critical value of Ra_0, since the difference between the peaks is too large, only $n = n_1''$ rough peak having the height of h_1'' are in contact with the friction pair. Therefore, it is concluded that the actual contact peak number n of the MRE has an inverse relationship with the relative roughness rate k_0, which can be expressed as:

$$n = \lambda_1 \frac{n_0}{k_0} + \lambda_2 = \lambda_1 \frac{n_0 Ra_0}{Ra} + \lambda_2 \tag{2}$$

Where λ_1 and λ_2 are positive constants, the number of constants is determined by the actual contact situation. Due to MRE is a kind of viscoelastic material, the contact problem with the friction pair of copper block during the sliding friction test can be converted into the contact

between a plurality of elastic spheres which have a radius of curvature R and elastic modulus of E with a rigid plane, as shown in Figure 9.

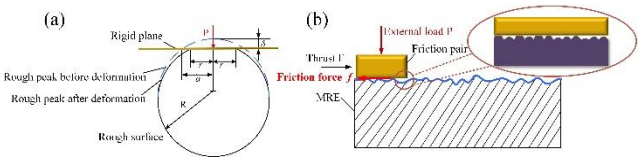

Figure 9 Analysis of controllable sliding friction characteristics of MRE: (a) schematic diagram of surface roughness peak contact; (b) schematic diagram of surface friction process of MRE

When the rough surface is pressed by the external load P and the rigid friction pair, the deformation due to the extrusion first occurs between the higher roughness peaks. The stress state of the single rough peak is analyzed, as shown in Figure 9(a). As shown in the picture, the actual contact state of the rough peak changes from a broken line to a solid line, and the actual contact area is a circle with a radius r. The actual contact area between the single rough peak and the friction pair is derived by the analysis of the elastic mechanic equation [28]:

$$A_1 = \pi r^2 = \pi \left(\frac{3PR}{4E}\right)^{2/3} \tag{3}$$

However, the actual rough surface of the MRE is composed of a large number of rough peaks of different height, and during the contact process. Plurality of rough peaks is simultaneously involved in the contact. Therefore, the actual contact area between the MRE and the rigid friction pair is also related to the number of contact roughness peaks. Assuming that the number of surface peaks of the MRE in contact with the rigid friction pair is n under a certain pressure, the actual contact area of the surface of the MRE can be expressed as:

$$A_0 = n\pi r^2 = n\pi \left(\frac{3PR}{4E}\right)^{2/3} \tag{4}$$

When the MRE comes into contact with the friction pair, the friction force is generated under a certain thrust force, and the friction force can be considered as the sum of the mechanical action and the molecular action of contacting the rough peak [26]. According to the actual contact area derived, the friction force of the surface of the MRE can be determined as [29, 30]:

$$f = \alpha A_0 + \beta P = \alpha \left[n\pi \left(\frac{3PR}{4E}\right)^{2/3}\right] + \beta P \tag{5}$$

Where α and β are constants, the number of constants is determined by the physical and mechanical properties of the surface of the MRE. It can be seen from the equation that the surface friction force of the MRE under a certain pressure is related to the elastic modulus E and affected by the number n of contact peaks. In the previous study [24], it was found that the MRE samples with different initial morphology will have different changes in surface morphology under an external applied magnetic field. The sample with a relatively smooth initial surface under the magnetic field, has an increased surface roughness and a large difference in height between the rough peaks. Conversely, the sample with a relatively rough initial surface under the magnetic field, has a decreased surface roughness and a small difference in height between the rough peaks. How the change in surface topography of the MRE under the magnetic field will affect the number of contact peaks, and the surface friction force will be further analyzed.

Taking equation (2) into equation (5), and the friction force of the surface of the MRE is further derived as follows:

$$f = \alpha A_0 + \beta P = \alpha \left[\left(\lambda_1 \frac{n_0 Ra_0}{Ra} + \lambda_2\right) \pi \left(\frac{3PR}{4E}\right)^{2/3}\right] + \beta P \tag{6}$$

It can be seen from equation (6) that the change of the surface friction force of the MRE mainly depends on the change of the surface roughness and the elastic modulus. By adjusting the degree of change of these two important parameters, the effective control of the surface friction force of the MRE can be achieved.

In general, the change rate of the elastic modulus of MRE under magnetic field is relatively high, which can increase 123% [26]. Although the surface morphology of the MRE is also controlled by the magnetic field to produce changes [24], compared with the changes in the elastic modulus, the range of surface morphology changes is smaller, which only within 30%. Since λ_1 and λ_2 are positive constants, the influence degree of elastic modulus is greater than that of surface roughness, so the changing trend of MRE friction force mainly depends on the magnetic-controlled elastic modulus, and the influence of magnetic-controlled surface morphology is relatively small. Combined with the previous experimental analysis under certain assumptions and ideal conditions, the changing trend among the friction force, the surface roughness and elastic modulus was obtained, as shown in Table 3. The variation range of the friction force drop was roughly obtained based on the experimental data. Based on that the positive pressure force does not change, and then the degree of change in friction is equivalent to the degree of change in friction coefficient. The analysis shows that the variation of the magnetic-controlled friction coefficient is influenced by the coupling between surface roughness and elastic modulus. The reduction of the friction coefficient of MRE is mainly due to the observable increase in the magnetic-controlled elastic modulus. Affected by the change of the magnetic-controlled surface roughness, the

friction coefficient of the S-MREs is reduced more than that of the R-MREs.

Table 3 Analysis of magnetic-controlled sliding friction mechanism of MRE

Samples	Magnetic-controlled surface morphology	Magnetic-controlled elastic modulus	Sliding friction force expression	Influence degree of reduced friction force
Smooth initial surface	The surface roughness increased↑	elastic modulus increased↑	$f = \alpha A_0 + \beta P = \alpha\left[\left(\lambda_1 \frac{n_0 R a_0}{Ra} + \lambda_2\right)\pi\left(\frac{3PR}{4E}\right)^{2/3}\right] + \beta P$	Large (10%-23%)
Rough initial surface	The surface roughness reduced↓	elastic modulus increased↑		Small (1%-10%)

Both theoretical analysis and experimental tests show that the magnetic-controlled sliding friction characteristics of MREs is determined by two important factors: surface roughness and elastic modulus, and the elastic modulus plays a decisive role. By adjusting those two factors, the frictional characteristics of MREs can be accurately controlled. It is beneficial to promote the engineering application of MREs with controllable sliding friction characteristics.

4 Conclusions

(1) The sliding friction tests which regard MRE and copper block as friction pair were carried out on samples with different initial surface roughness. The experimental results show that the sliding friction coefficient of MRE decreases with the increase of the magnetic field, but the degree of reduction is quite different under different initial surface roughness and elastic modulus. The maximum change rate in S-MREs is 22.75% of sample 3, and sample 8 which has the largest change rate in R-MREs is only 9.04%. It is found that the frictional properties of MREs under the magnetic field are affected by surface roughness and elastic modulus. Moreover, change features of elastic modulus and surface topography under magnetic field were tested and analyzed. The elastic modulus of S-MREs and R-MREs both increased with the enhancement of a magnetic field, and the surface roughness of S-MREs was the same trend, but the surface roughness of R-MREs reduced when the magnetic field increased. Therefore, the friction coefficient of the S-MREs has a greater range of variation, and the R-MREs have a small change range of friction coefficient. When the initial surface roughness of MRE is between 0.5 - 2.5 μm and the ferromagnetic particles volume fraction is between 10% - 15%, its magnetic-controlled friction coefficient change range is the largest, which can be reduced by about 23%.

(2) Under the condition of ignoring the influence of some other mechanical properties, and combined with the single peak contact model and the friction binomial law, the relationship between the surface roughness and elastic modulus of MREs and the sliding friction force is deduced. The results proved that the friction coefficient is mainly affected by the coupling effect of surface roughness and elastic modulus. It can be seen that the magnetic-controlled elastic modulus is the key factor, and the change rate of the elastic modulus is relatively large, which determines the overall downward trend of the friction coefficient of MREs. Although the surface roughness is not decisive, the magnetic-controlled surface roughness also plays an important role in the adjustable range of friction coefficient, and reducing the initial surface roughness can expand the magnetic-controlled friction coefficient adjustable range. The theoretical analysis results are consistent with the experimental data. To obtain better magnetic-controlled sliding friction characteristics, the elastic modulus of MRE can be large, and the initial surface roughness should be as small as possible. By adjusting the changes of the two influencing factors, it can help to research and promote the engineering application of MREs controllable sliding friction characteristics and interfacial contact fields.

5 Declaration

Acknowledgements

The authors sincerely thanks to Professor Wang Xiaojie, a researcher at the Institute of Advanced Manufacturing Technology of the Hefei Institute of Chinese Academy of Sciences for the helpful comments in writing and revising to improve the paper. The authors sincerely thanks to Professor ** for his critical discussion and reading during manuscript preparation.

Funding

Supported by National Nature Science Foundation of People's Republic of China (No. 52075063), the Science and Technology Research Program of Chongqing Municipal Education Commission (KJZD-K201900602), the Special Key Project of Technological Innovation and Application

Development in Chongqing (cstc2019jscx-fxydX0085), and the Science and technology research project of Chongqing Municipal Education Commission (No. KJQN201800644)

Availability of data and materials

The datasets supporting the conclusions of this article are included within the article.

Competing interests

The authors declare no competing financial interests.

Consent for publication

Not applicable

Ethics approval and consent to participate

Not applicable

References

[1] C Y Min. Z B He. H Y Liang. D D Liu. C K Dong. H J Song. Y D Huang. High mechanical and tribological performance of polyimide nanocomposite reinforced by fluorinated graphene oxide. *Polymer Composites*, 2020, 41(4): 1624-1635.

[2] O Hod. E Meyer. Q S Zheng. M Urbakh. Structural superlubricity and ultralow friction across the length scales. *Nature*, 2018, 563(7732): 485-492.

[3] H Fu. G P Yan. M Li. H Wang. Y P Chen. C Yan. C T Lin. N Jiang. J H Yu. Graphene as a nanofiller for enhancing the tribological properties and thermal conductivity of base grease. *RSC Advances*, 2019, 9(72): 42481-42488.

[4] Q W Huang. H G Liu. Z Ding. Dynamical response of the shaft-bearing system of marine propeller shaft with velocity-dependent friction. *Ocean Engineering*, 2019, 189(1): 106399.

[5] N Singh. Y Singh. A Sharma. A Singla. Effect of addition of copper nanoparticles on the tribological behavior of macadamia oil at different sliding speeds. *Energy Sources Part A-Recovery Utilization and Environmental Effects*, 2019, 41(23): 2917-2928.

[6] B Y Lee. D H Kim. J Park. K I Park. K. J Lee. C K Jeong. Modulation of surface physics and chemistry in triboelectric energy harvesting technologies. *Science and Technology of Advanced Materials*, 2019, 20(1): 758-773.

[7] X H Zhan. P Yi. Y C Liu. P F Xiao. X Y Zhu. J Ma. Effects of single- and multi-shape laser-textured surfaces on tribological properties under dry friction. *Proceedings of the Institution of Mechanical Engineers Part C-Journal of Mechanical Engineering Science*, 2020, 234(7): 1382-1392.

[8] B Acharya. C M Seed. D W Brenner. A I Smirnov. J Krim. Tuning friction and slip at solid-nanoparticle suspension interfaces by electric fields. *Scientific Reports*, 2019, 9(1): 18584.

[9] Y Wang. Y Zhang. C Tang. J Yu. H He. H Qi. Solid/liquid interfacial friction and slip behaviors on roughness surface under applied voltage. *Tribology International*, 2020, 144(1): 106128.

[10] J Zhao. Q Li. S Li. S Li. G Chen. X Liu. Y He. J Luo. Influence of a carbon-based tribofilm induced by the friction temperature on the tribological properties of impregnated graphite sliding against a cemented carbide. *Friction*, 2020, https://doi.org/ 10.1007/s40544-019-0358-3.

[11] X B Nguyen. T Komatsuzaki. N Zhang. A nonlinear magnetorheological elastomer model based on fractional viscoelasticity, magnetic dipole interactions, and adaptive smooth Coulomb friction. *Mechanical Systems and Signal Processing*, 2020, 141(1): 106438.

[12] S Lee. C Yim. W Kim. S Jeon. Magnetorheological elastomer films with tunable wetting and adhesion properties. *ACS Applied Materials & Interfaces*, 2015, 7(35): 19853-19856.

[13] M A Cantera. M Behrooz. R F Gibson. F Gordaninejad. Modeling of magneto-mechanical response of magnetorheological elastomers (MRE) and MRE-based systems: a review. *Smart Materials and Structures*, 2017, 26(2): 023001.

[14] X Y Gu. Y Yu. Y C Li. J C Li. M Askari. B Samali. Experimental study of semi-active magnetorheological elastomer base isolation system using optimal neuro fuzzy logic control. *Mechanical Systems and Signal Processing*, 2019, 119(1): 380-398.

[15] Y Tao. X T Rui. F F Yang. B L Hao. Development of a MRE isolation system for strapdown inertial measurement unit. *Mechanical Systems and Signal Processing*, 2019, 117(1): 553-568.

[16] S Yarra. F Gordaninejad. M Behrooz. G Pekcan. A M Itani. N Publicover. Performance of a large-scale magnetorheological elastomer-based vibration isolator for highway bridges. *Journal of Intelligent Material Systems and Structures*, 2018, 29(20): 3890-3901.

[17] D W Lee. K Lee. C H Lee. C H Kim. W O Cho. A study on the tribological characteristics of a magneto-rheological elastomer. *Journal of Tribology-Transactions of the ASME*, 2013, 135(1): 014501.

[18] C L Lian. K H Lee. C H Lee. Friction and wear characteristics of magneto-rheological elastomers based on silicone/polyurethane hybrid. *Journal of Tribology-Transactions of the ASME*, 2015, 137(3): 031607.

[19] R Li. D J Ren. X J Wang. X Chen. S W Chen. X Wu. Tunable friction performance of magneto-rheological elastomer induced by external magnetic field. *Journal of Intelligent Material Systems and Structures*, 2018, 29(2): 160-170.

[20] R Li. X Li. P A Yang. J S Liu. S C Chen. The field-dependent surface roughness of magnetorheological elastomer: numerical simulation and experimental verification. *Smart Materials and Structures*, 2019, 28(8): 085018.

[21] C L Lian. K H Lee. C H Lee. Friction and wear characteristics of magnetorheological elastomer under vibration conditions. *Tribology International*, 2016, 98(1): 292-298.

[22] T Kawasetsu. T Horii. H Ishihara. M Asada. Mexican-Hat-Like Response in a Flexible Tactile Sensor Using a Magnetorheological Elastomer. *Sensors*, 2018, 18(2): 587.

[23] M D Christie. S S Sun. D H Ning. H Du. S W Zhang. W H Li. A torsional MRE joint for a C-shaped robotic leg. *Smart Materials and Structures*, 2017, 26(1): 015002.

[24] R Li. X Li. Y Y Li. P A Yang. J S Liu. Experimental and numerical study on surface roughness of magnetorheological elastomer for controllable friction. *Friction*, 2020, 8(5): 917-929.

[25] Z Geng. T M Shao. Microstructure and tribological behavior of stripe patterned Ti0.6Al0.4N thin coatings prepared by masked deposition. *Surface & Coatings Technology*, 2015, 283(1): 364-372.

[26] S W Chen. R Li. Z Zhang. X J Wang. Micromechanical analysis on tensile modulus of structured magneto-rheological elastomer. *Smart Materials and Structures*, 2016, 25(3): 035001.

[27] M Nosonovsky. B Bhushan. Multiscale friction mechanisms and hierarchical surfaces in nano- and bio-tribology. *Materials Science &*

Engineering R-Reports, 2007, 58(3-5): 162-193.
[28] X Yin. K Komvopoulos. A slip-line plasticity analysis of abrasive wear of a smooth and soft surface sliding against a rough (fractal) and hard surface. *International Journal of Solids and Structures*, 2012, 49(1): 121-131.
[29] S Z Wen. P Huang. *Principles of tribology. 3rd ed.*. Beijing: Tsinghua University Press. 2008. (in Chinese)
[30] Z Shi. Z Jin. X Guo. X Shi. J Guo. Interfacial friction properties in diamond polishing process and its molecular dynamic analysis. *Diamond and Related Materials*, 2019, 100(1): 107546.

Biographical notes

Rui Li, born in 1975, is currently a PhD candidate at *Chongqing University, China*. His current position is a professor in *Chongqing University of Posts and Telecommunications*. His main research interests include intelligent detection technology, friction control and intelligent mechanical structure system.
Tel: +86-135-94078659; E-mail: lirui_cqu@163.com

Di Wang, born in 1996, is currently a master candidate at *School of Automation, Chongqing University of Posts and Telecommunications, China*.
E-mail: 812996901@qq.com

Xinyan Li, born in 1995, is currently a master candidate at *School of Automation, Chongqing University of Posts and Telecommunications, China.*
E-mail: 459148593@qq.com

Ping-an Yang, born in 1989, is currently a PhD candidate at *Chongqing University, China*. His current position is a lecturer in *Chongqing University of Posts and Telecommunications*. His main research interests include intelligent biomimetic composite materials, flexible sensor, electromagnetic shielding material and structural design.
Tel: +86-151-23254645; E-mail: yangpa@cqupt.edu.cn

Haibo Ruan, born in 1984, is currently a PhD candidate at *Chongqing University, China*. His research interests include construction of flexible nanowire composite transparent electrode and its performance enhancement.
Tel: +86-136-47619849; E-mail: rhbcqu@aliyun.com

Mengjie Shou, born in 1993, is currently a PhD candidate at *Chongqing University, China*. His main research interests include intelligent detection technology, friction control and intelligent mechanical structure system.
E-mail: shoumj@cqupt.edu.cn

Figures

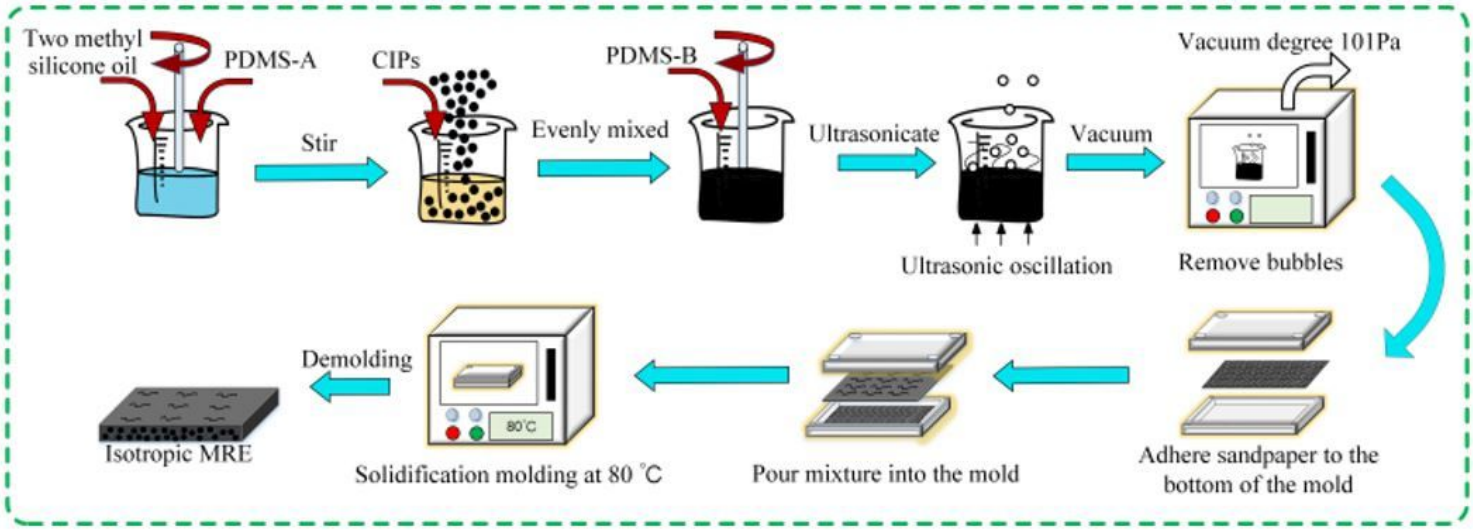

Figure 1

The preparation process of isotropic MRE samples with different roughness

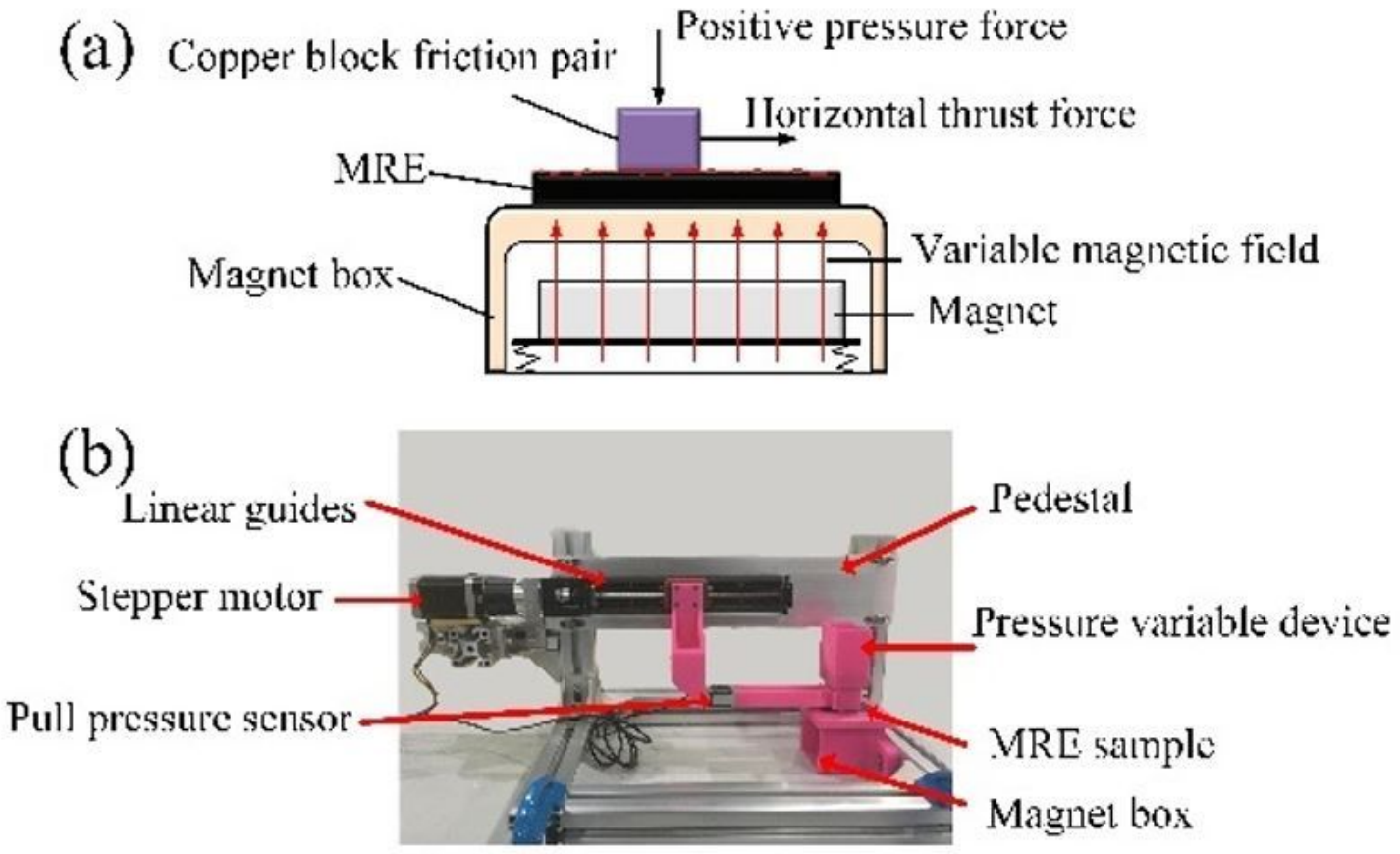

Figure 2

Measurement principle of MRE sliding friction characteristics and physical diagram of platform: (a) Schematic diagram of sliding friction test; (b) MRE sliding friction test platform

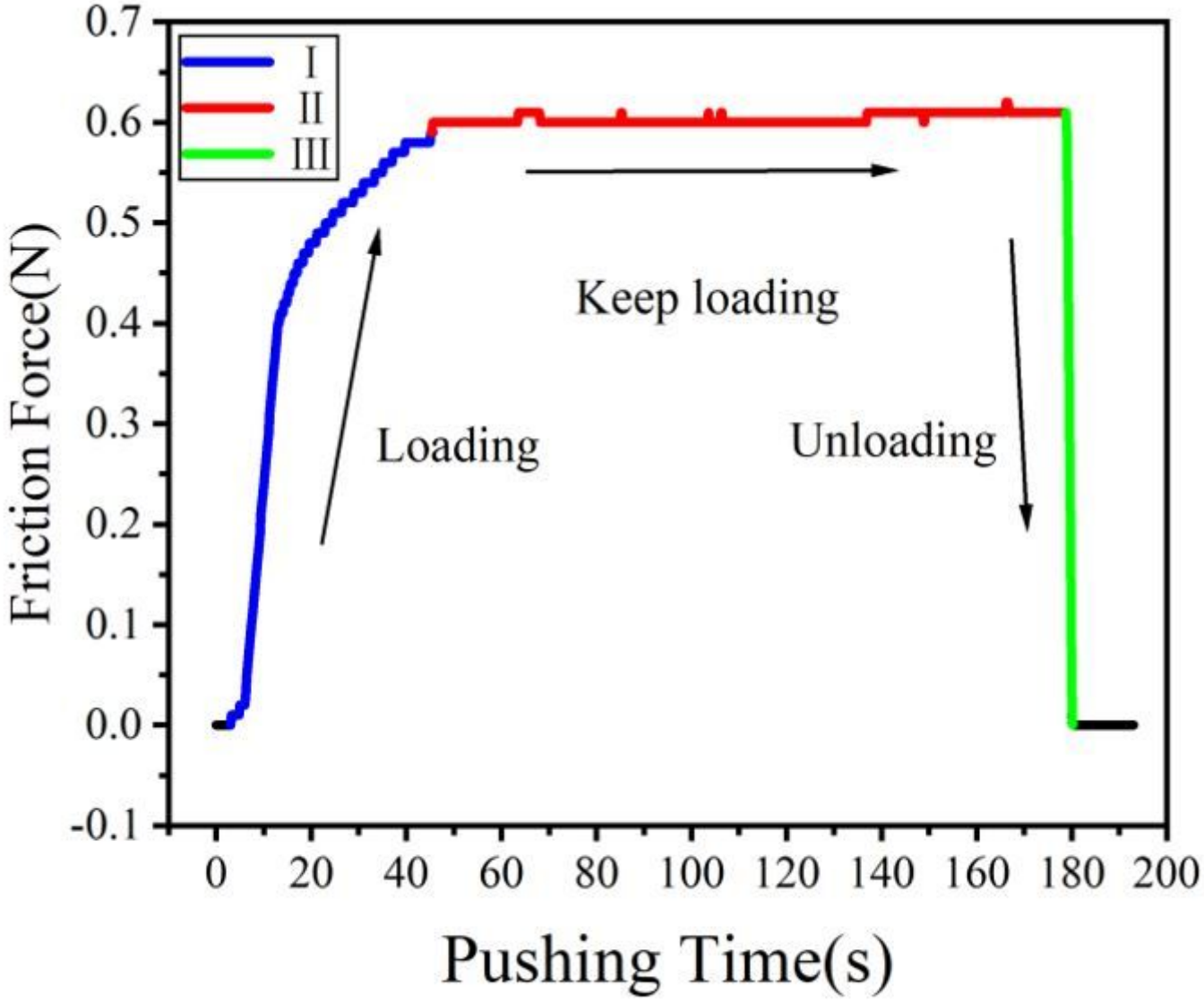

Figure 3

Pushing time and friction force curve of sample 7 when the positive pressure is 0.95 N: (□) Loading period; (□) Keep loading period; (□)Unloading period

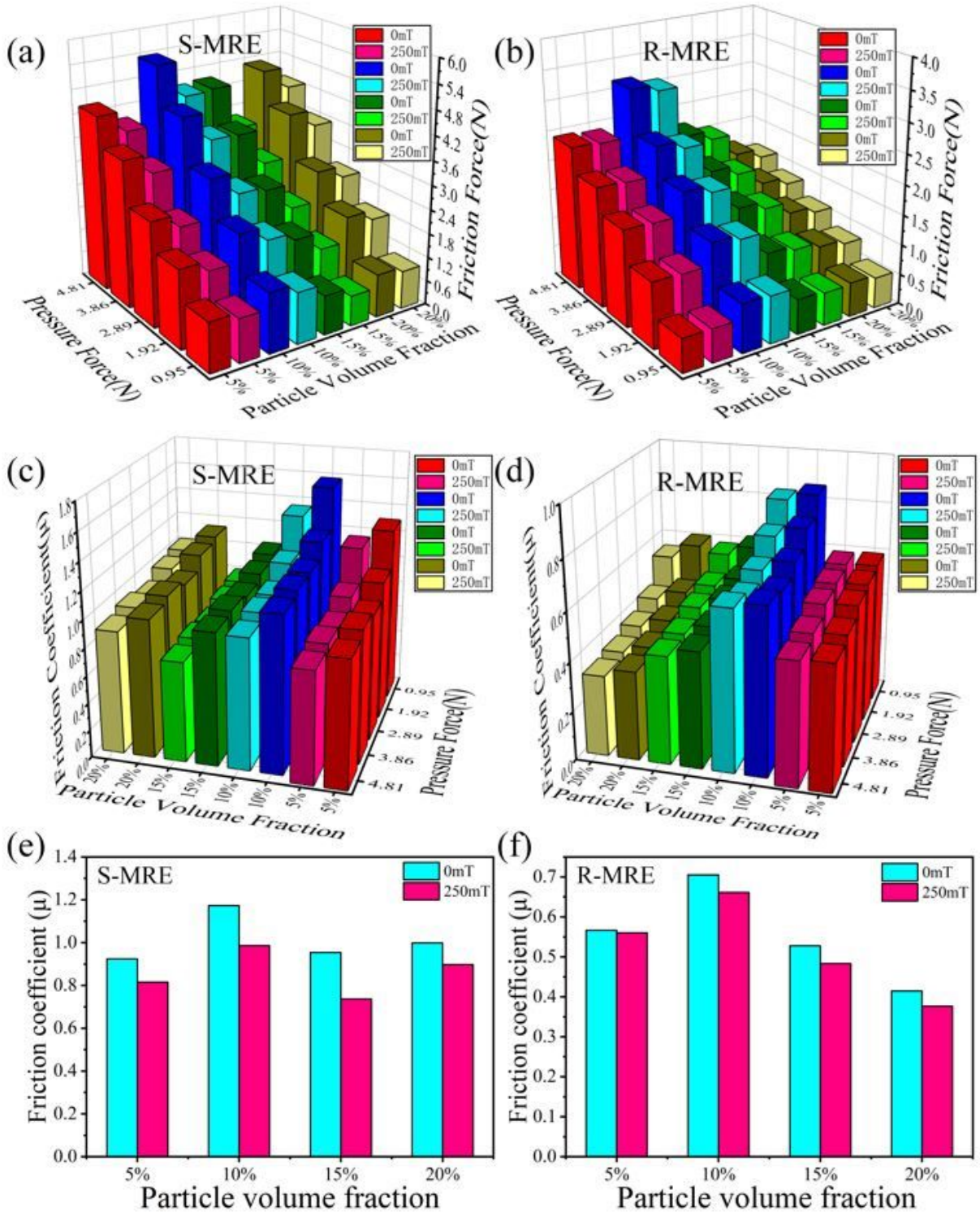

Figure 4

Results of MRE friction experiments with different roughness: (a) Friction force of S-MRE samples; (b) Friction force of R-MRE samples; (c) Friction coefficient of S-MRE samples; (d) Friction coefficient of R-MRE samples; (e) Friction coefficient of S-MRE samples when the positive pressure is 2.89 N; (f) Friction coefficient of R-MRE samples when the positive pressure is 2.89 N

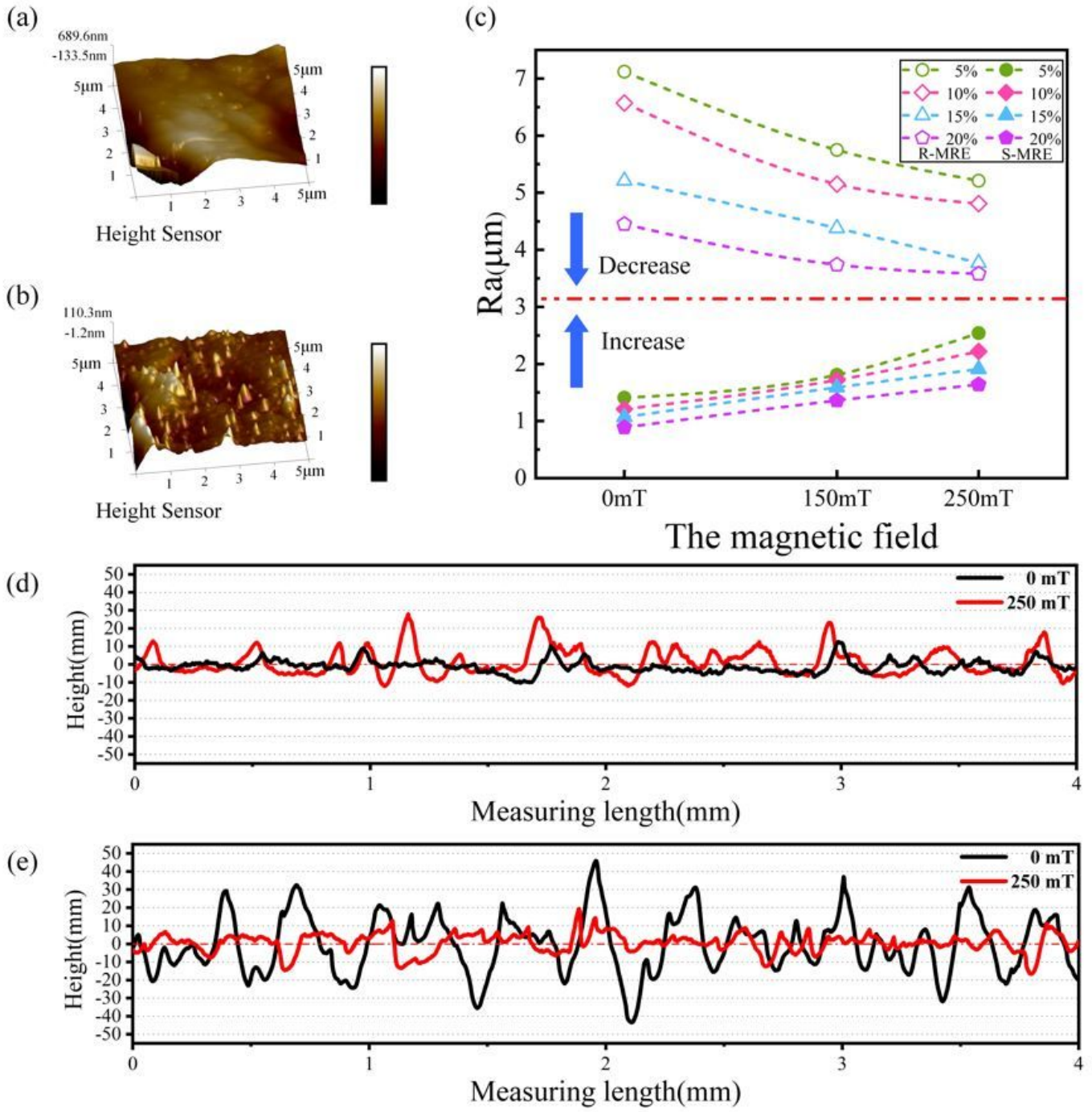

Figure 5

Surface profile comparison of MREs with different surface roughness: (a) AFM of S-MRE sample 2; (b) AFM of R-MRE sample 6; (c) Comparison of surface roughness changes of MRE samples 1-8 under magnetic field; (d) One-dimensional contour change of S-MRE sample 2 under magnetic field; (e) One-dimensional contour change of R-MRE Sample 6 under magnetic field

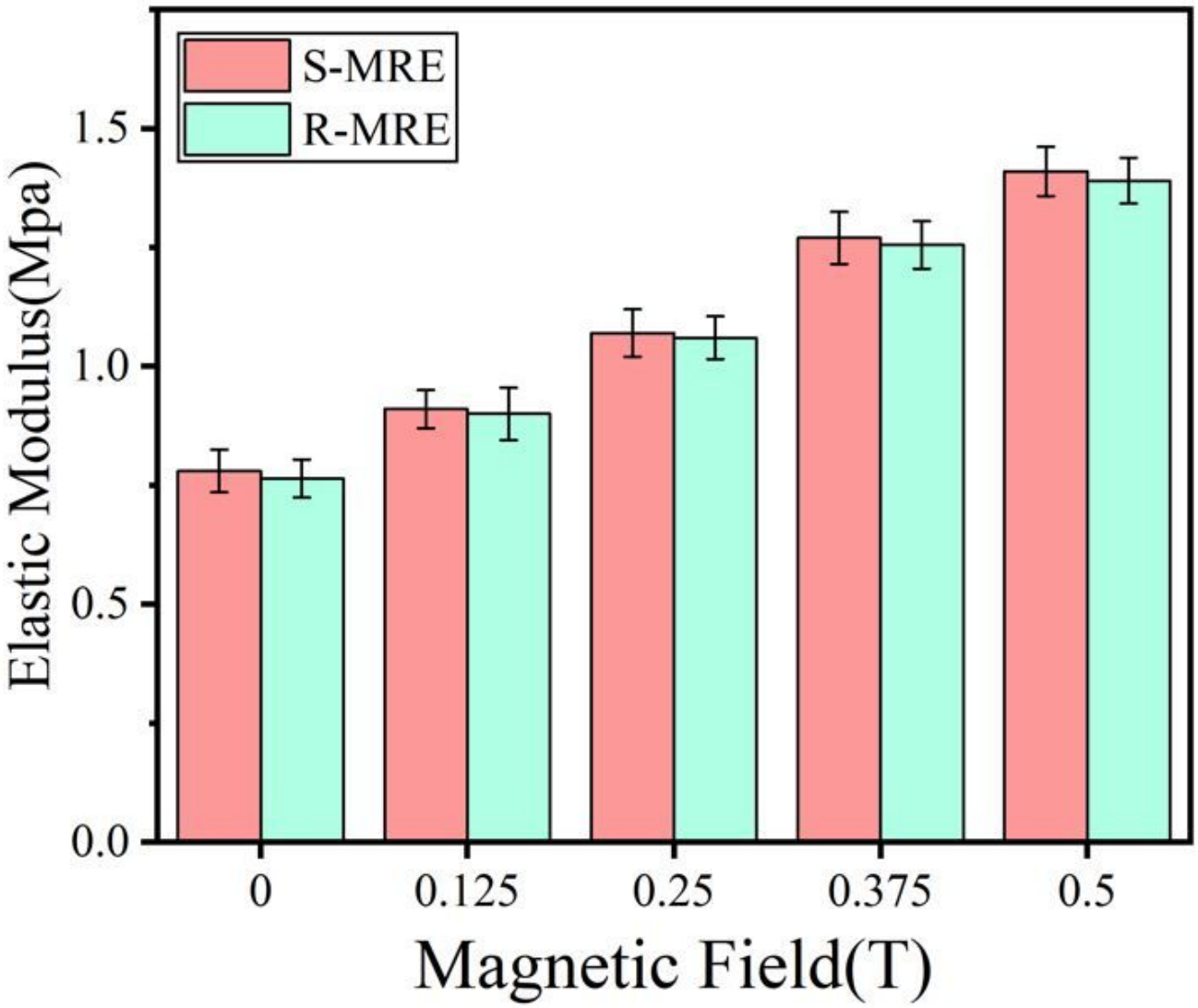

Figure 6

Elastic modulus of MRE samples 2 and 6 with different surface roughness

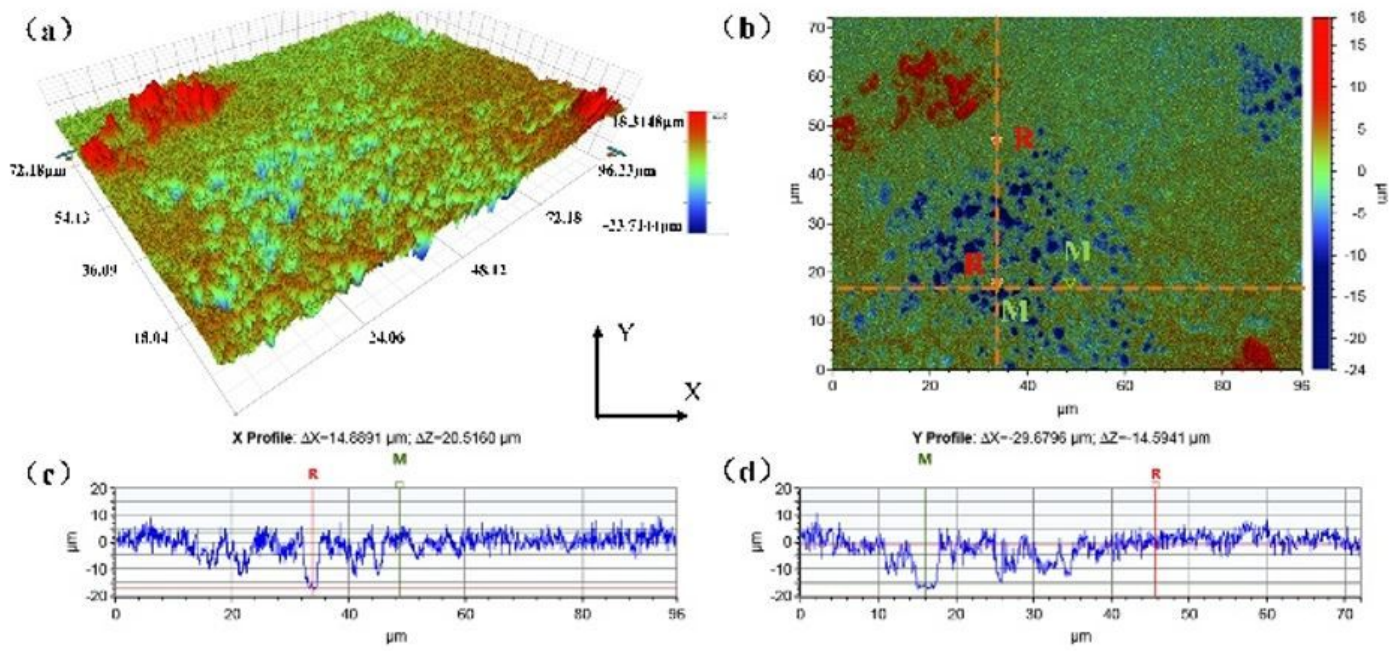

Figure 7

Observation results of surface morphology of MRE: (a) three-dimensional surface topography of MRE; (b) two-dimensional surface topography of MRE; (c) contour curve of MRE along the x-direction; d) contour curve of MRE along the y-direction

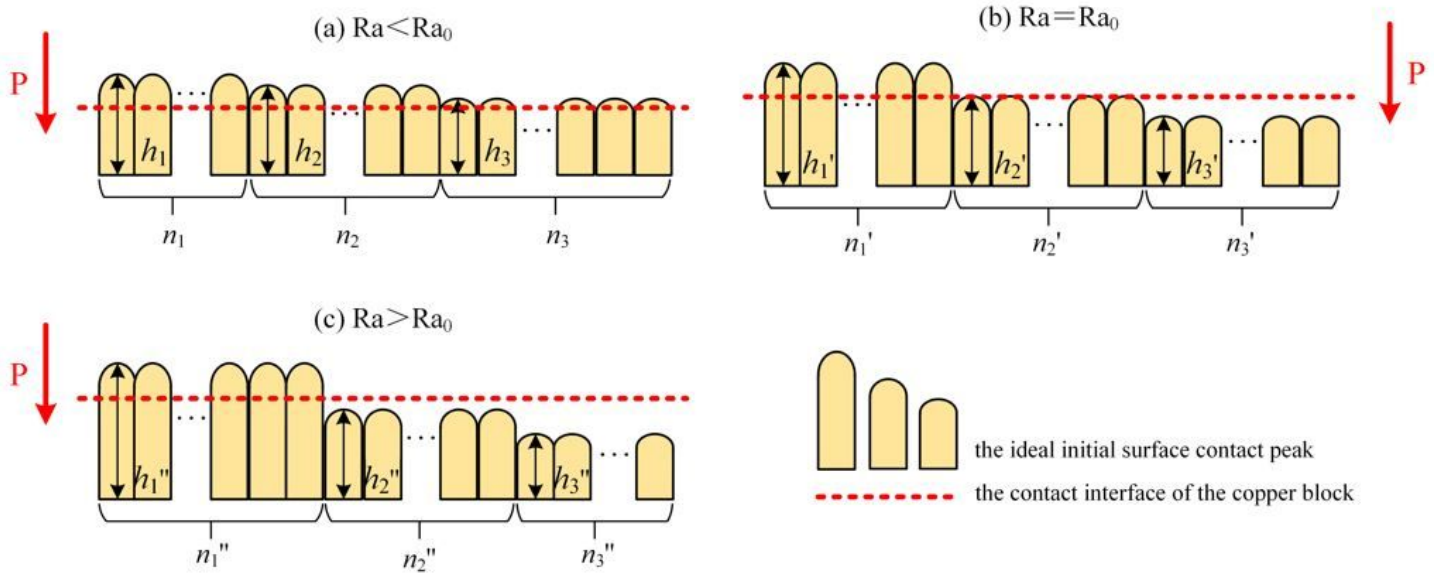

Figure 8

The different contact diagram of the ideal initial surface morphology of MRE and the surface of the copper block when pressed

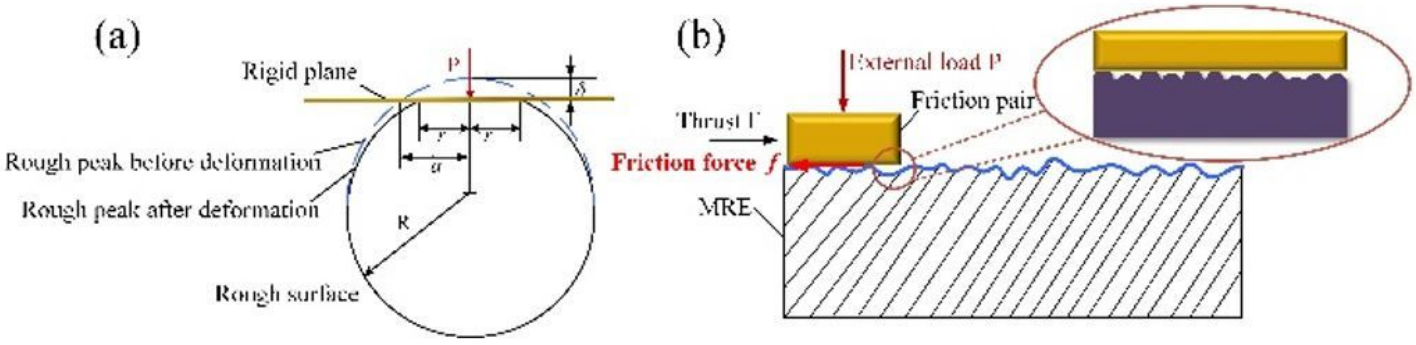

Figure 9

Analysis of controllable sliding friction characteristics of MRE: (a) schematic diagram of surface roughness peak contact; (b) schematic diagram of surface friction process of MRE